Liquid Crystals
Publication details, including instructions for authors and subscription information:
http://www.informaworld.com/smpp/title~content=t713926090

Phase behaviour under pressure of a dichiral liquid crystal with an optically isotropic cubic phase: 2-{4-[(*R*)-2-fluorohexyloxy]phenyl}-5-{4-[(*S*)-2-fluoro-2-methyldecanoyloxy]phenyl}pyrimidine

Yoji Maeda[a]; Hiroshi Yokoyama[a]; Atsushi Yoshizawa[b]; Tetsuo Kusumoto[c]
[a] Liquid Crystal Nano-system Project, SORST, Japan Science and Technology Agency, Tsukuba, Ibaraki 300-2635, Japan [b] Department of Materials Science and Technology, Faculty of Science and Technology, Hirosaki University, Hirosaki 036-8561, Japan [c] Liquid Crystal Materials Division, Dainippon Ink & Chemicals, Inc., Saitama 362-8577, Japan

To cite this Article Maeda, Yoji , Yokoyama, Hiroshi , Yoshizawa, Atsushi and Kusumoto, Tetsuo(2007) 'Phase behaviour under pressure of a dichiral liquid crystal with an optically isotropic cubic phase: 2-{4-[(*R*)-2-fluorohexyloxy]phenyl}-5-{4-[(*S*)-2-fluoro-2-methyldecanoyloxy]phenyl}pyrimidine', Liquid Crystals, 34: 1, 9 — 18
To link to this Article: DOI: 10.1080/02678290600905412
URL: http://dx.doi.org/10.1080/02678290600905412

Liquid Crystals, Vol. 34, No. 1, January 2007, 9–18

Phase behaviour under pressure of a dichiral liquid crystal with an optically isotropic cubic phase: 2-{4-[(*R*)-2-fluorohexyloxy]phenyl}-5-{4-[(*S*)-2-fluoro-2-methyldecanoyloxy]phenyl}pyrimidine

YOJI MAEDA*†, HIROSHI YOKOYAMA†, ATSUSHI YOSHIZAWA‡ and TETSUO KUSUMOTO§

†Liquid Crystal Nano-system Project, SORST, Japan Science and Technology Agency, TRC 5-9-9 Tokodai, Tsukuba, Ibaraki 300-2635, Japan

‡Department of Materials Science and Technology, Faculty of Science and Technology, Hirosaki University, 3 Bunkyo-cho, Hirosaki 036-8561, Japan

§Liquid Crystal Materials Division, Dainippon Ink & Chemicals, Inc., 4472-1 Komuro, Ina-machi, Kitaadachi-gun, Saitama 362-8577, Japan

(*Received 21 March 2006; accepted 25 April 2006*)

The phase behaviour of a dichiral liquid crystalline compound with an optically isotropic cubic phase, 2-{4-[(*R*)-2-fluorohexyloxy]phenyl}-5-{4-[(*S*)-2-fluoro-2-methyldecanoyloxy]-phenyl}pyrimidine, (*R*,*S*)-FPPY, was investigated under pressures up to 100 MPa using a polarizing optical microscope equipped with a high pressure optical cell and a high pressure differential thermal analyser. (*R*,*S*)-FPPY exhibits the isotropic liquid (I)–chiral smectic C (SmC*)–optically isotropic cubic (Cub)–chiral smectic X (SmX*)–crystal (Cr) transition sequence on cooling at pressures up to about 13 MPa, in which the SmC*–Cub transition occurs with an associated endothermic peak. The heating process of the (*R*,*S*)-FPPY crystals showed the Cr–SmX*–Cub–I and Cr–SmX*–SmC*–I phase sequences under pressures below and above about 50 MPa, respectively. The triple point for the SmX*, Cub and isotropic liquid phases was estimated to be about 52 ± 1 MPa, 143.0 ± 0.5°C, indicating the upper limit of pressure for the formation of the cubic phase. On the other hand, the phase behaviour of (*R*,*S*)-FPPY in the cooling mode changed drastically at pressures above 13–14 MPa: after the I–SmC* transition, the SmC* phase remained without the SmC*–Cub transition on cooling, but the subsequent heating showed the SmC*–Cub–I phase sequence in the intermediate pressure region between 14 and about 50 MPa, and the reversible SmC*–I transition in the high pressure region. It is concluded that the cubic phase appears reversibly in the low pressure region and appears only on heating in the intermediate pressure region, but that it disappears completely in the high pressure region. The SmC* phase is thermodynamically metastable at low pressures below 50 MPa and is stable at higher pressures.

1. Introduction

The phase behaviour of 2-{4-[(*R*)-2-fluorohexyloxy]-phenyl}-5-{4-[(*S*)-2-fluoro-2-methyldecanoyloxy]phenyl}-pyrimidine, referred to as (*R*,*S*)-FPPY, has been attracting much attention because of the formation of an optically isotropic phase and the occurrence of endothermic transition from the ferroelectric chiral smectic C phase (SmC*) to the optically isotropic cubic (Cub) phase in the cooling mode [1]. (*R*,*S*)-FPPY exhibits the phase transition sequence of isotropic liquid (I)–SmC*–Cub–chiral smectic X* (SmX*)–crystal (Cr) on cooling under atmospheric pressure, in which the SmC*–Cub transition is accompanied by an endothermic heat of transition (table 1). Surprisingly the chiral SmC* phase does not appear on the subsequent heating and the Cr–SmX*–Cub–I phase sequence is observed with a much higher Cub–I transition temperature. The molecular formula of (*R*,*S*)-FPPY is:

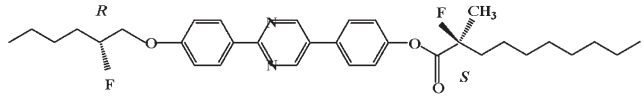

the diastereomers of (*R*,*S*)-FPPY, (*R*,*R*) and (*S*,*S*), do not show the optically isotropic cubic phase, but the racemic mixture of the two enantiomers does exhibit the cubic phase [1]. Furthermore slight modification of the molecular structure, except for the terminal chain

*Corresponding author. Email: maeda@nanolc.jst.go.jp

Liquid Crystals
ISSN 0267-8292 print/ISSN 1366-5855 online © 2007 Taylor & Francis
http://www.tandf.co.uk/journals
DOI: 10.1080/02678290600905412

Table I. Thermodynamic quantities associated with the phase transitions of (*R*,*S*)-FPPY.

Transition	*T*/°C	ΔH/kJ mol^{-1}	ΔS/J mol^{-1}
Heating mode			
Cr–SmX*	90.2	20.5	56.4
SmX*–Cub	95.9	4.0	10.9
Cub–I	128.3	3.1	7.7
Cooling mode			
I–SmC*	114.0	−2.1	−5.5
SmC*–Cub	112.6	0.6	1.5
Cub–SmX*	91.8	−3.2	−8.9
SmX*–Cr	68.9	−12.9	−37.8

lengths, depresses the cubic phase [2, 3]. Thus these property–structure correlations suggest strongly that the cubic phase is organized by chiral molecular recognition. The transition behaviour of a binary mixture between (*R*,*S*)-FPPY and (*R*,*R*)-FPPY with a phase sequence of I–SmC*–SmX* varied with the composition in the heating and cooling modes [4]. The phase behaviour of the mixture with the (*R*,*R*)-FPPY content more than 45 wt% did not show the cubic phase on cooling; a triple point for the SmC*, Cub and SmX phases was found between 40 and 45 wt% (*R*,*R*)-FPPY. The transition behaviour of another binary mixture between (*R*,*S*)-FPPY and the corresponding monochiral liquid crystal, 2-{4-[hexyloxy]phenyl}-5-4-{[(*S*)-2-fluoro-2-methylnonanoyl]phenyl}pyrimidine (II) with a phase sequence of I–SmC*–SmX*–Cr also varied with composition in the heating and cooling modes [5]. Thermal hysteresis in transitional behaviour in the cooling and heating modes was observed in a mixture of (*R*,*S*)-FPPY (75 wt%) and II (25 wt%), and the cubic phase appeared only during heating. The thermal behaviour of (*R*,*S*)-FPPY, observed using a high resolution a.c. calorimeter [6], showed that the I–SmC* phase transition was anomalous and exhibited a quite different behaviour. A new transitional feature in the isotropic phase was found, corresponding to a very broad peak of heat capacity over a 30 K temperature range. Such strange but intriguing phase behaviour of (*R*,*S*)-FPPY prompted us to study the effect of pressure on the phase transition behaviour, especially the SmC*–Cub phase transition on cooling and the phase stability of the optically isotropic cubic phase itself.

In this paper we report the interesting results of the morphological and thermal behaviour of (*R*,*S*)-FPPY under hydrostatic pressures up to 120 MPa using a polarizing optical microscope equipped with a high pressure optical cell and a high pressure differential thermal analyser.

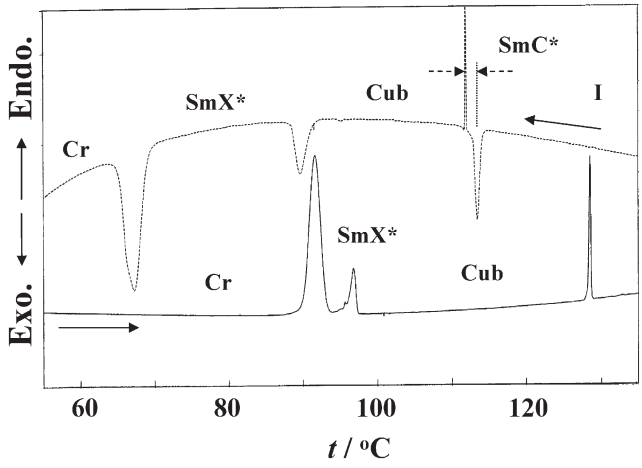

Figure 1. DSC cooling and subsequent heating curves of (*R*,*S*)-FPPY. Scanning rate: 2°C min^{-1}.

2. Experimental

2.1. *Sample preparation and characterization*

The (*R*,*S*)-FPPY sample used in this study was prepared as described elsewhere [2]. The sample was characterized using a Perkin-Elmer Pyris1 differential scanning calorimeter (DSC) and a Leitz Orthoplan polarizing optical microscope (POM) equipped with a Mettler hot stage FP-82. DSC measurements were performed at a scanning rate of 2°C min^{-1} under N_2 gas flow. Temperatures and heats of transition were calibrated using indium and tin standards. Transition temperatures were determined as the onset of the transition peaks at which the tangential line of the inflection point of the rising part of the peak crosses over the extrapolated baseline.

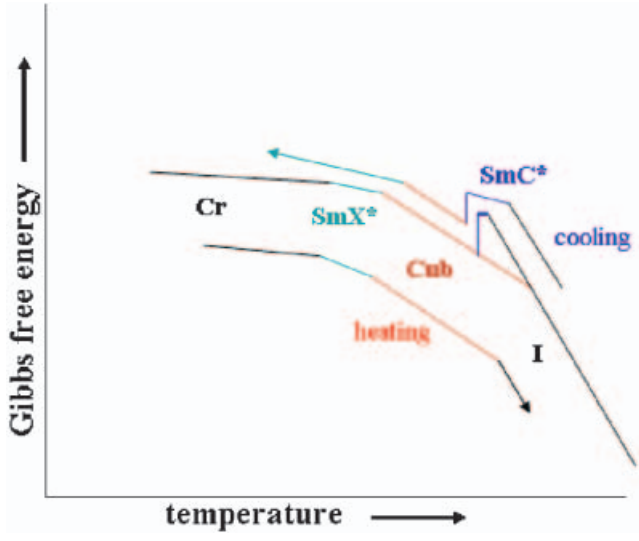

Scheme I

2.2. *Morphological and DTA measurements under pressure*

The texture observation of (*R*,*S*)-FPPY under hydrostatic pressure was performed using a Leitz Orthoplan POM equipped with a high pressure optical cell system with sapphire windows, as described elsewhere [7]. The high pressure DTA apparatus used in this study is described elsewhere [8, 9]; it was operated in a temperature region between room temperature and

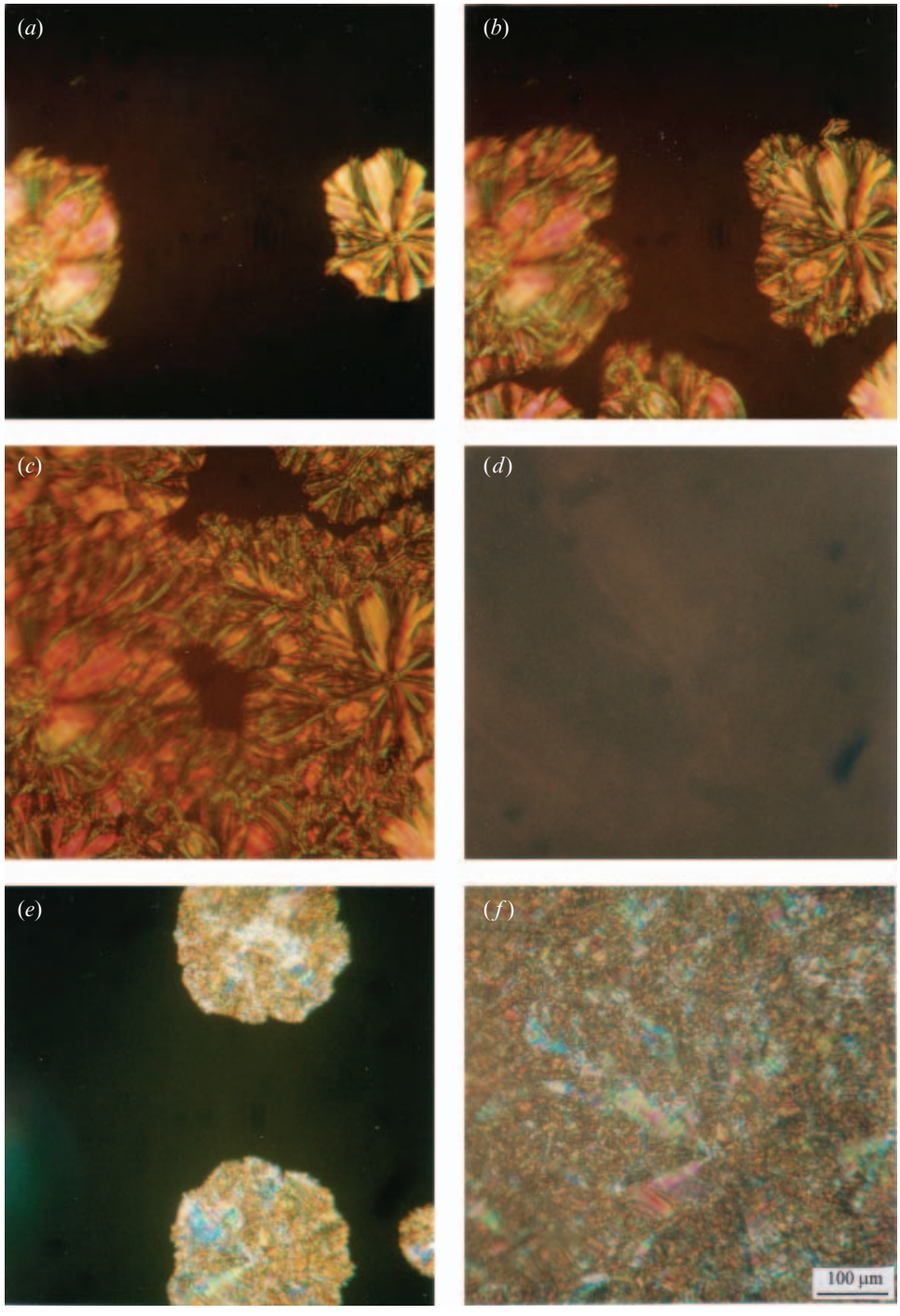

Figure 2. POM photographs of texture of (*R*,*S*)-FPPY on cooling from the isotropic liquid at atmospheric pressure: (*a*,*b*) flower-like texture of the ferroelectric chiral SmC* phase at 114°C; (*c*) SmC* phase at 113°C; (*d*) Cub phase at 112°C; (*e*, *f*) SmX* phase at 92 and 80°C, respectively.

180°C under hydrostatic pressures up to 150 MPa. Dimethylsilicone oil with a medium viscosity (100 cSt) was used as the pressurizing medium. A sample of about 4 mg was placed inside the sample cell, which was coated with epoxy adhesive to fix the sample in the cell and also to prevent direct contact with the silicone oil. The DTA runs were performed at a constant scanning rate of $4^{\circ}C\,min^{-1}$ under various pressures. Peak temperatures were taken as the transition temperatures for constructing the temperature vs. pressure phase diagram.

3. Results and discussion

Figure 1 shows the DSC cooling and subsequent heating curves of (*R*,*S*)-FPPY at a scanning rate of $2^{\circ}C\,min^{-1}$. On cooling, (*R*,*S*)-FPPY exhibits the I–SmC*–Cub–SmX*–Cr phase sequence at atmospheric pressure, in which the SmC*–Cub transition occurs with an endothermic peak [1]. The Cr–SmX*–Cub–I phase sequence is observed on subsequent heating, showing the Cub–I transition at a much higher temperature. The phase sequence of (*R*,*S*)-FPPY in cooling and heating modes at atmospheric pressure is shown below [1].

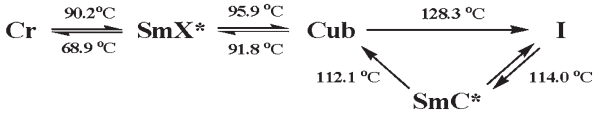

The SmC* phase appears as a monotropic phase on cooling from the isotropic liquid and then transforms into the stable cubic phase. The phase relations are understood qualititatively using the Gibbs free energy vs. temperature diagram shown in scheme 1 [2].

Figure 2 shows the POM textures of (*R*,*S*)-FPPY on cooling from the isotropic liquid at atmospheric pressure. The flower-like texture of the chiral SmC* phase was formed at 114°C from the isotropic liquid, figures 2 (*a*) and 2 (*b*), and the texture was seen in full at 113°C, figure 2 (*c*). The texture then disappeared abruptly into a black field of view for the optically isotropic cubic phase at 112°C, figure 2 (*d*). The dark field of view for the cubic phase was held on cooling until the texture of a smectic, undetermined (SmX*) phase appeared at 92°C, figure 2 (*e*), and then the SmX* phase expanded gradually on cooling, figure 2 (*f*).

Figures 3 (*a*) and 3 (*b*) show the typical texture of the SmC* phase grown largely in the isotropic liquid at 11 MPa, which shows a concentric-circles texture inside the petals of flowers with diameters over 100 µm. The concentric-circles texture seems to reflect the helical structure of the SmC* phase. When the hydrostatic pressure was raised to above about 14 MPa, the optically isotropic cubic phase did not appear in the cooling mode. So the flower-like concentric-circles texture of the SmC* phase was held at relatively low temperatures near 60°C on first cooling.

Figure 4 shows the POM textures of (*R*,*S*)-FPPY on cooling from the isotropic liquid at 20 MPa. The flower-like concentric-circles texture of the SmC* phase appeared at 123°C, figure 4 (*b*), in the isotropic liquid and then multiple concentric circles grew with decreasing temperature at 120, 92, and 50°C, figures 4 (*c–e*), respectively. The texture observation of (*R*,*S*)-FPPY on cooling under higher pressures showed only the I–SmC* transition and the resultant textures for the SmC* phases remained at lower temperatures. On the subsequent heating of the SmC* phase at 20 MPa, an interesting phase behaviour was observed. Figures 5 (*a–c*) show the POM textures of the SmC* phase on the subsequent heating at 20 MPa. One can see the change in texture from the concentric-circles texture of the SmC* phase at 90°C, figure 5 (*a*), via the SmC*–Cub transition at 108°C, figure 5 (*b*), to the cubic phase at 109°C, figure 5 (*c*), on the subsequent heating. Here the optically isotropic cubic phase appeared only on heating at 20 MPa, which means that the cubic phase is still

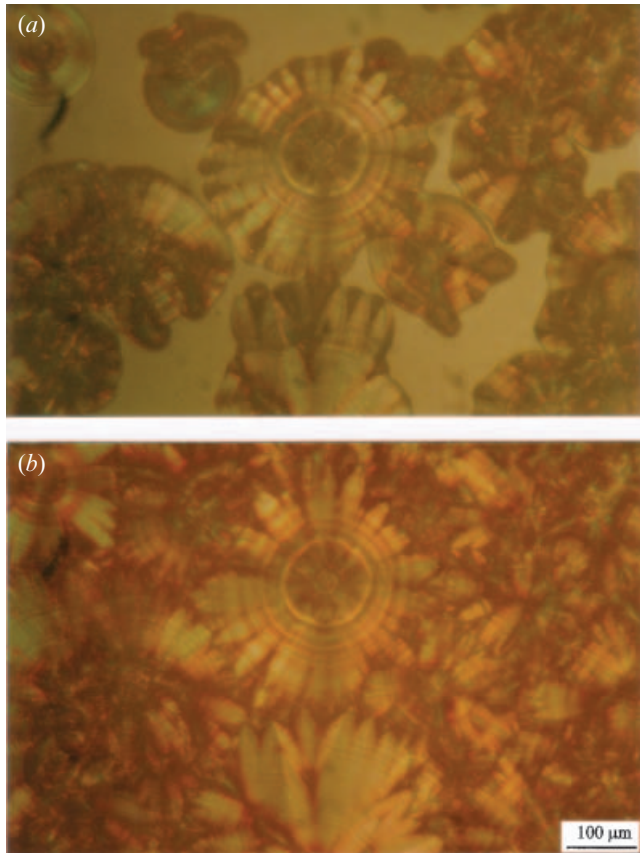

Figure 3. Sunflower-like, concentric circular texture of the ferroelectric chiral SmC* phase on cooling at 11 MPa: (*a*) 118°C, (*b*) 110°C.

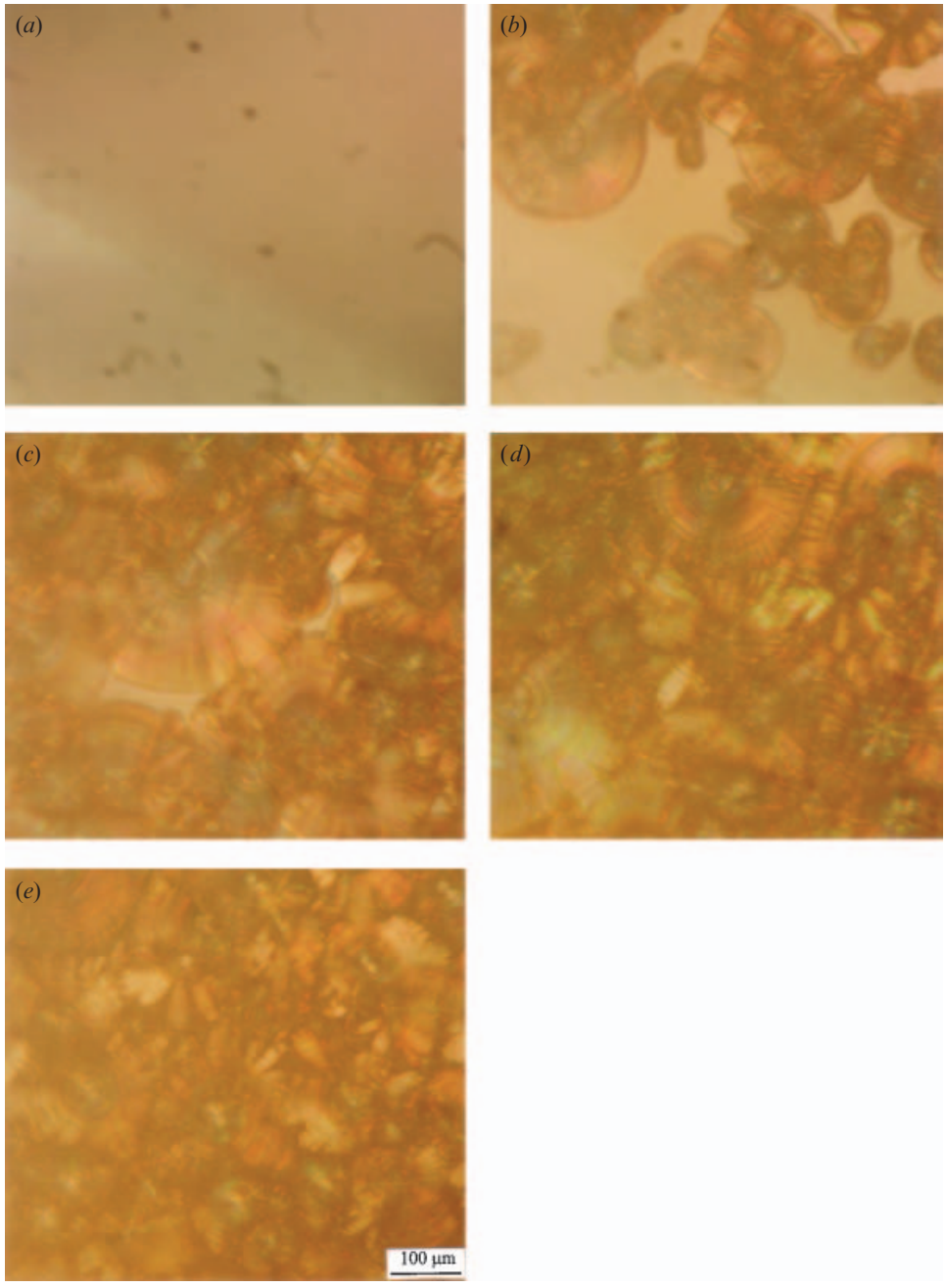

Figure 4. POM photographs of texture of (*R*,*S*)-FPPY on cooling from the isotropic liquid at 20 MPa: (*a*) isotropic liquid at 130°C; (*b*) concentric circular textures of the SmC* phase at 123°C; (*c*,*d*,*e*) SmC* phase at 120, 92 and 50°C, respectively.

thermodynamically stable. Figures 5 (*d–f*) show the POM textures of the sample on the successive cooling from the cubic phase at 20 MPa. This shows the formation of another texture, clearly different from that of the SmC* phase. Optically anisotropic, dark lumps appeared in the cubic phase at 104 and 103°C, figures 5 (*d*) and 5 (*e*), and these grew to give the typical texture for the SmX* phase at 102°C, figure 5 (*f*): i.e. the Cub–SmX* transition occurred on the successive cooling at 20 MPa. This interesting change of texture in this thermal cycling was observed also at 30 MPa.

The phase behaviour of (*R*,*S*)-FPPY in the cooling mode is summarized as follows. There are three pressure regions in the phase behaviour: first is the I–SmC*–Cub–SmX*–Cr phase sequence on first cooling in the low pressure region below 13–14 MPa, in which

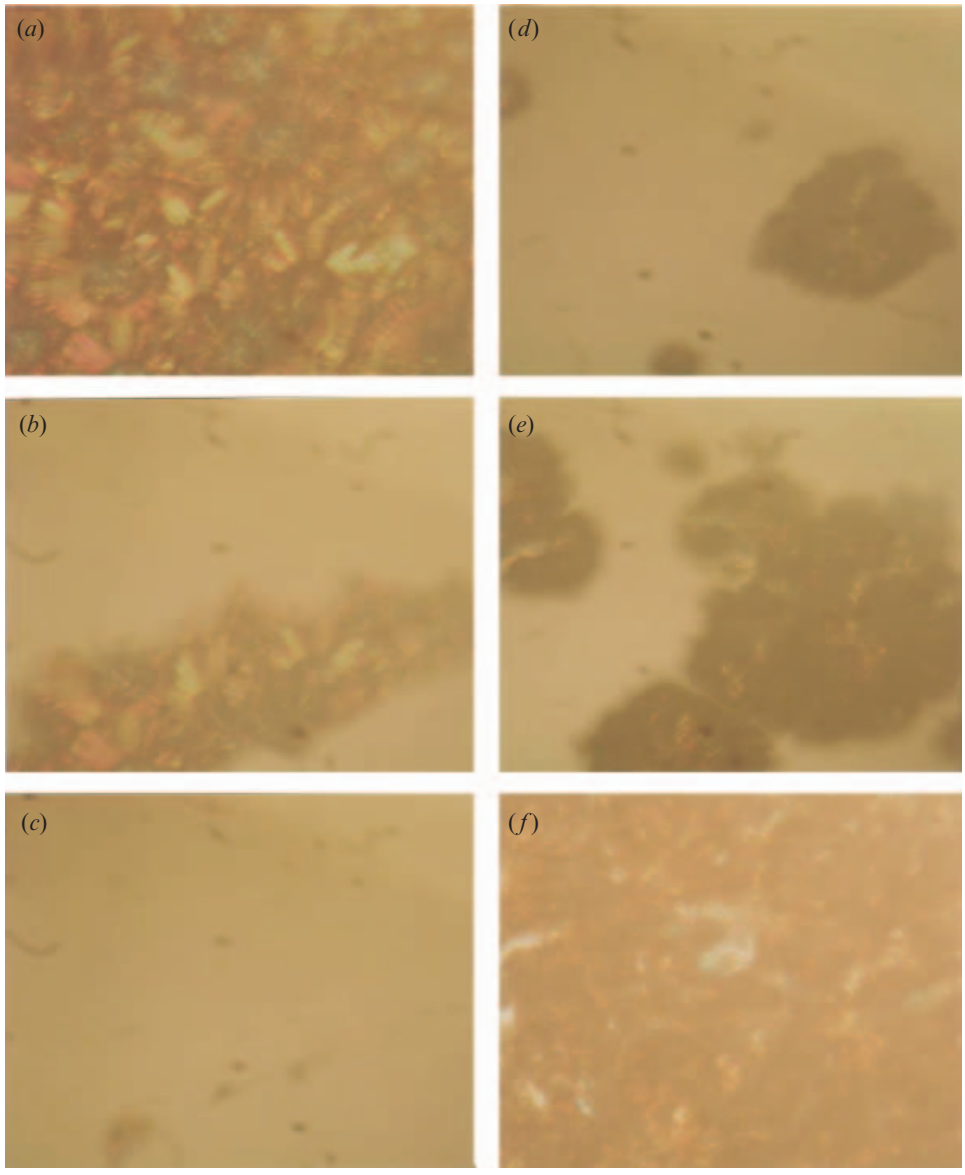

Figure 5. Texture change of the SmC* phase on the 2nd heating and succeeding cooling from the cubic phase at 20 MPa: (*a*) SmC* phase at 90°C; (*b*) SmC*–Cub transition at 108°C; (*c*) Cub phase at 109°C on heating; (*d*,*e*) Cub–SmX* transition at 104 and 103°C on the succeeding cooling; and (*f*) SmX* phase at 102°C.

the monotropic SmC* phase is formed between the isotropic liquid and the cubic phase, and the cubic phase is reversibly observed. Interestingly the temperature region of the SmC* phase broadens rapidly with increasing pressure, due to the negative slope (dT/dP) of the SmC*–Cub transition, while the temperature range of the cubic phase decreases. The SmX* and Cr phases are formed successively with decreasing temperature.

Second is the intermediate pressure region between 14 and about 50 MPa, in which only the I–SmC* transition is observed on first cooling but the SmC*–Cub–I transition sequence appears on the subsequent heating. When the SmC* phase was cooled to the presumably supercooled SmC* phase at relatively low temperatures and then reheated, the supercooled SmC* phase was transformed into the cubic phase, similarly to the usual SmX*–Cub transition. The most striking feature in the intermediate pressure region is that the cubic phase does not appear on cooling, while it appears on heating. This strange behaviour is reported in the (*R*,*S*)-FPPY and (*R*,*R*)-FPPY binary mixture with 45 and 47.5 wt% of (*R*,*R*)-FPPY composition; the I–SmC*–SmX phase sequence was observed on cooling, while the

smectic–Cub–I transition sequence was detected on the subsequent heating; i.e. the cubic phase appears only on heating in the boundary region [4]. Furthermore when the cubic phase was cooled again, the same Cub–SmX*–Cr transition, as the later part of the I–SmC*–Cub–SmX*–Cr phase sequence in the low pressure region, was observed at 30 MPa. So the I–(1st cooling)–SmC*–(2nd heating)–Cub–(2nd cooling)–SmX* phase sequence could be observed during this thermal cycling.

Thermal cycling is requited for the stable phase sequence because the cubic phase does not appear on cooling under intermediate pressures. It is noted that the cubic phase is a key for the appearance of the later phase sequence (Cub–SmX*–Cr) in the intermediate pressure region. This phase behaviour can be understood using the criteria of Gibbs free energy shown in scheme 1. We consider that the cubic phase shifts sensitively to its higher energy levels with increasing pressure, suggesting a movement toward the instability of the cubic phase. The energy difference between the cubic and SmC* phases decreases on applying pressure, compared with that at atmospheric pressure shown in scheme 1. Accordingly the SmC* phase will be easily supercooled along the its own energy line without the SmC*–Cub transition. The I–SmC*–(supercooled SmC*) phase sequence is preferentially observed on first cooling in the intermediate pressure region.

Third is the high pressure region above about 50 MPa, in which the Cr–SmX*–SmC*–I phase sequence on heating but the I–SmC*–(supercooled SmC*) phase sequence on cooling are observed. The cubic phase disappears completely in the high pressure region. The texture observation of (*R*,*S*)-FPPY on cooling and heating at 70 MPa showed reversibly the I–SmC* transition. The texture change during the SmC*–I transition occurred gradually in a relatively wide temperature range between 145 and 152°C at 70 MPa. Figure 6 shows schematically the phase behaviour of (*R*,*S*)-FPPY in the cooling mode under hydrostatic pressures up to 100 MPa. For the save of clarity, the intermediate pressure region, the SmX*–Cub and Cub–I transition lines for the stable cubic phase in the heating mode are added as broken red lines.

Figure 7 shows DTA heating curves of the as-prepared sample of (*R*,*S*)-FPPY under hydrostatic pressure. They show three endothermic peaks for the Cr–SmX*, SmX*–Cub, and Cub–I transitions under pressure. The SmX*–Cub transition shifted significantly to higher temperatures with increasing pressure. The thermal behaviour for the Cr–SmX*–Cub–I phase sequence agreed well with POM texture observation in the pressure range up to 50 MPa. The DTA curves at higher pressures above 70 MPa showed only two peaks

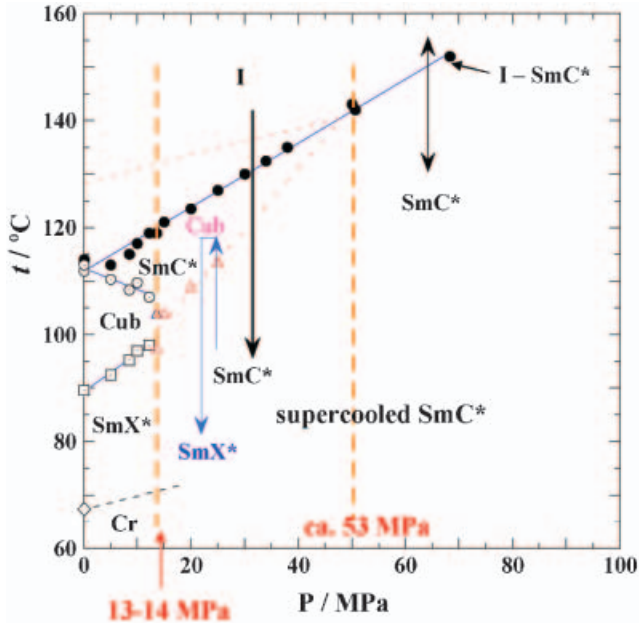

Figure 6. Schematic *T* vs. *P* phase diagram of (*R*,*S*)-FPPY constructed in the cooling mode. The phase behaviour is different in the low, intermediate and high pressure regions. Blue lines in the intermediate pressure region exhibit the SmC*–Cub–SmX* transition during the 2nd heating and successive cooling via the cubic phase. The area inside the red broken lines represents the cubic phase observed in the heating mode.

corresponding to the melting (Cr–SmX* transition) and an undetermined transition, respectively.

Unfortunately the SmC*–I transition could not be detected at high temperatures, probably due to the low sensitivity of the high pressure DTA. Based on the thermal and morphological phase behaviour of (*R*,*S*)-FPPY, the *T* vs. *P* phase diagram constructed in the heating mode is shown in figure 8. The Cr–SmX*–Cub–I phase sequence was observed at pressures up to about 50 MPa. The transition curves can be expressed approximately as either first or second order polynomials in order of pressure:

(*t*/°C: peak temperature)

Transition	*whole pressures*	
Cr→SmX*	$T=91.9+0.324_3\ (P/\mathrm{MPa})-4.92_6\times10^{-4}\ (P/\mathrm{MPa})^2$ $0<P<52$ MPa	(by DTA)
SmX*→Cub	$T=97.6+0.245_8\ (P/\mathrm{MPa})+1.28_6\times10^{-2}\ (P/\mathrm{MPa})^2$	(by POM)
Cub→I	$T=130.8+0.249_0\ (P/\mathrm{MPa})$ $52\ \mathrm{MPa}<P$	(by DTA)
SmC*→I	$T=112.6+0.591_8\ (P/\mathrm{MPa})$	(by POM)

The temperature region of the SmX* phase broadens with increasing pressure, while that of the cubic

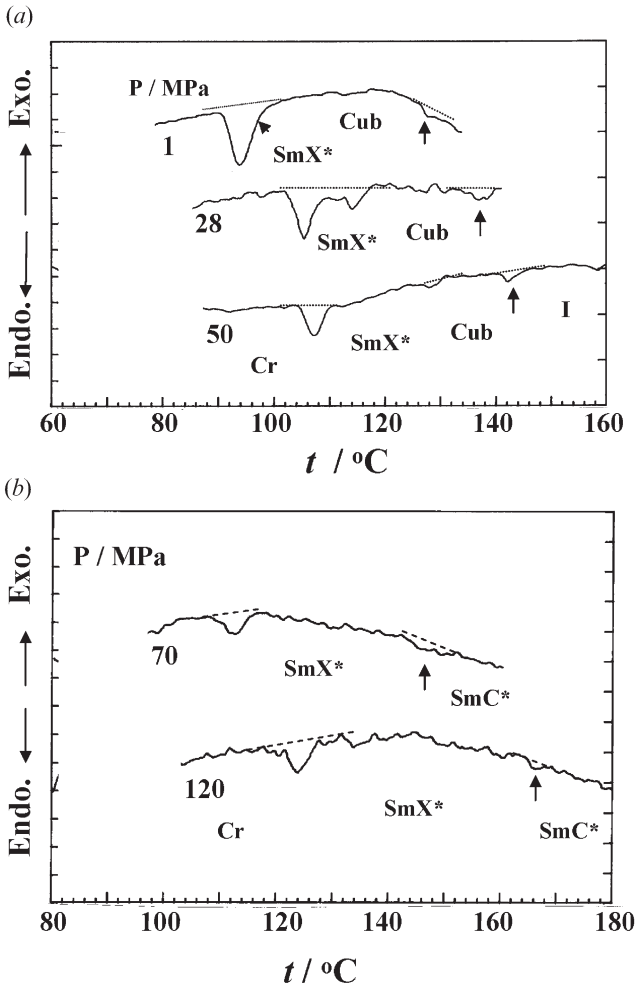

Figure 7. High pressure DTA heating curves of the as-prepared sample of (*R*,*S*)-FPPY. Heating rate: 4°C min^{-1}.

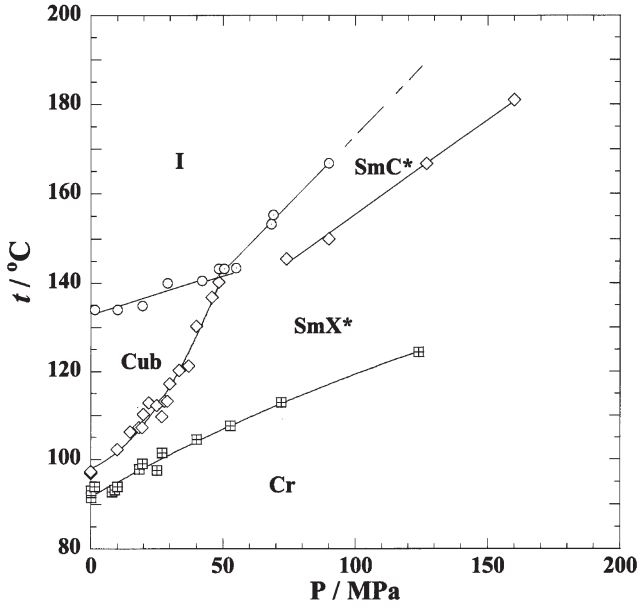

Figure 8. *T* vs. *P* phase diagram of the (*R*,*S*)-FPPY crystalline sample in the heating mode. The black and red lines were estimated using the DTA and POM observations, respectively.

phase decreases. The SmX*–Cub transition curve rises rapidly with increasing pressure and finally merges with the Cub–I transition lines at about 50 MPa. The triple point for the SmX*, cubic and isotropic liquid phases was estimated approximately to be 52 ± 1 MPa, 143.0 ± 0.5°C, indicating the upper limit of pressure for the formation of the cubic phase. Since the DTA heating curves of the crystals at high pressure showed the melting (Cr–SmX* transition) and an undetermined transition, and also the POM observations showed the reversible I–SmC* transition, the undetermined transition is reduced to be the SmX*–SmC* transition at higher pressures. Here we suggest the existence of the SmX*–SmC* transition in the mesophase region at higher pressures, schematically shown by a solid line in figure 8. The Cr–SmX*–SmC*–I transition will be a whole phase sequence at high pressures above about 52 MPa. The SmC* phase is stable in the high pressure region, while it is thermodynamically metastable in the low and intermediate pressure regions. Accordingly the phase behaviour of (*R*,*S*)-FPPY under pressure can be summarized in figure 9. It is emphasized that the cubic phase appears reversibly in the low pressure region between 0.1 and 13 MPa, but is observed only on heating in the intermediate pressure region. Further increase of pressure above about 52 MPa forced complete disappearance of the cubic phase.

It is interesting to see that the *T* vs. *P* phase diagram of (*R*,*S*)FPPY in this study closely resembles that of a binary mixture between (*R*,*S*)-FPPY and (*R*,*R*)-FPPY [4], and another binary mixture between (*R*,*S*)-FPPY and the corresponding monochiral liquid crystal 2-{4-[hexyloxy]phenyl}-5-4-{[(*S*)-2-fluoro-2-methylnonanoyl]-phenyl}pyrimidine (II), constructed in heating and cooling modes [5]. It is particularly noted that the phase behaviour of the cubic phase is very similar to that in figures 6 and 8 in this study, if the parameters of composition and pressure can be handled as exchangeable variables. The optically isotropic cubic phase is destabilized by applying pressure, similarly by adding the second component in a binary mixture. In the high pressure region with no appearance of the cubic phase, the SmC* phase in the (*R*,*S*)-FPPY single system will transform into the SmX* phase, such as in the transitions in the binary systems. It is interesting that the phase behaviour of the cubic phase and the

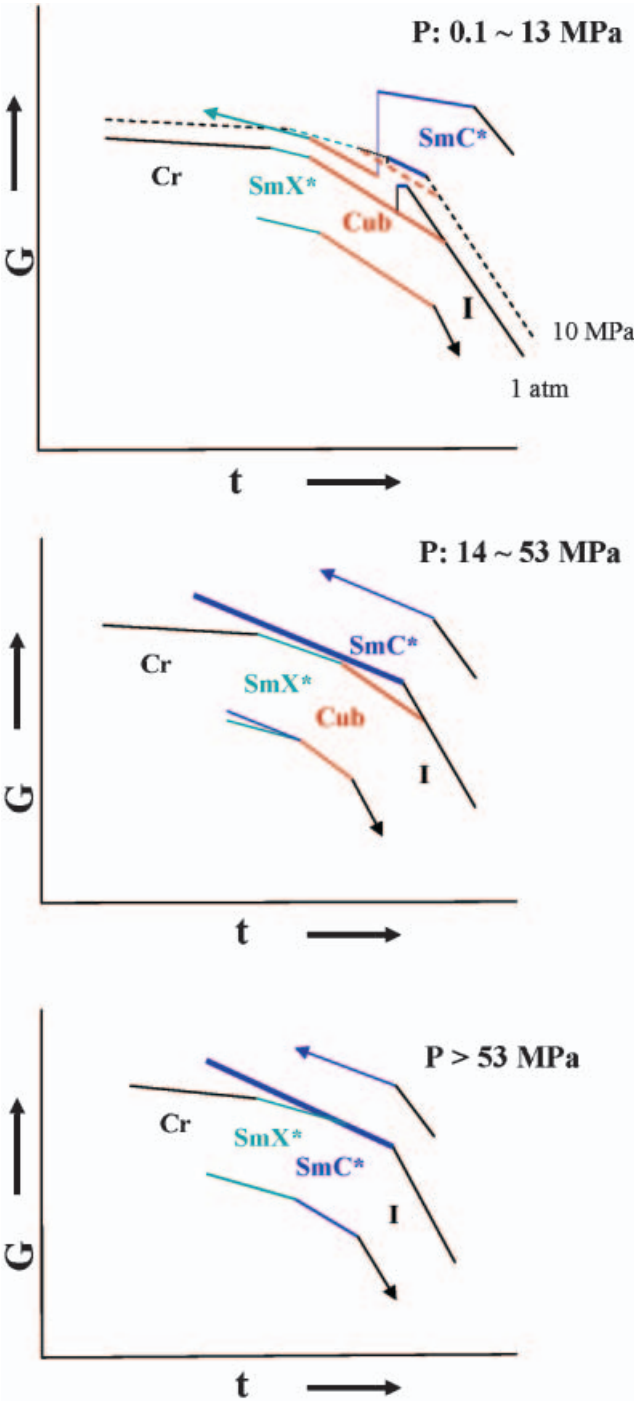

Figure 9. Gibbs free energy vs. temperature diagrams of (*R*,*S*)-FPPY in the three pressure regions.

existence of the triple point are very similar to those of 4′-*n*-hexadecyloxy-3′-nitrobiphenyl-4-carboxylic acid (ANBC-16) [10, 11].

The structure of the cubic phase was determined to have the symmetry group *I*432 by X-ray analysis [12]. The cubic phase emerging in the equimolar mixture of (*R*,*R*) and (*S*,*S*) stereoisomers also showed the *I*432 symmetry, indicating the formation of the cubic phase due to the chiral recognition between the chiral end chains. The crystal structure of (*R*,*S*)-FPPY was also determined by structure analysis [13]. The crystal has a smectic-like layer structure composed of four independent molecules. The molecular chains in the *b*-axis of the triclinic cell are parallel along the *c*-axis, but they are antiparallel along the *a*-axis. Strong interactions between the pyrimidine rings of antiparallel molecules is expected to lead to a large overlapping of the core moieties; also the strong interactions between the chiral groups are expected to reinforce each other. These expectations suggest that intralayer chirality-oriented electrostatic interaction contributes to the appearance of the cubic phase, while the SmC* phase has a helical structure caused by interlayer chiral twist interaction.

In summary, the cubic phase is destabilized by applying pressure, which is similar to the phase behaviour of thermotropic cubic mesogens ANBC-16 [10, 11] and 1,2-bis(4-*n*-octyloxy- and 1,2-bis(4-*n*-decyloxy-benzoyl)hydrazine (BABH-8 and BABH-10) [14, 15]. On the other hand, the formation of the ferroelectric chiral SmC* phase is kinetically predominant under high pressures above 14 MPa. It is concluded that the Cr–SmX*–Cub–I and Cr–SmX*–SmC*–I phase sequences of (*R*,*S*)-FPPY are stable in the low and high pressure regions, respectively. The SmC* phase appears on cooling under all pressures: it is metastable in the low and intermediate pressure regions, while it becomes stable at high pressures above about 52 MPa. This means that the chiral SmC* phase with helical structure is stable under pressures from the kinetic and thermodynamic points of view. On the other hand, the cubic structure with the pyrimidine rings of antiparallel molecules and strong intralayer chirality-oriented electrostatic interaction would be difficult to achieve under elevated pressures.

References

[1] A. Yoshizawa, J. Umezawa, N. Ise, R. Sato, Y. Soeda, T. Kusumoto, K. Sato, T. Hiyama, Y. Takanishi, H. Takezoe. *Jpn. J. appl. Phys.*, **37**, L942 (1998).

[2] T. Kusumoto, K. Sato, M. Katoh, H. Matsutani, A. Yoshizawa, N. Ise, J. Umezawa, Y. Takanishi, H. Takezoe, T. Hiyama. *Mol. Cryst. liq. Cryst.*, **330**, 227 (1999).

[3] A. Yoshizawa, N. Ise, T. Kusumoto, Y. Takanishi, H. Takezoe, T. Hiyama. *Mol. Cryst. liq. Cryst.*, **364**, 271 (2001).

[4] A. Yoshizawa, T. Kusumoto, Y. Takanishi, H. Takezoe, T. Hiyama. *Preprint of Annual Meeting of Japan Liquid Crystal Society*, 376–377 (1999).

[5] A. Yoshizawa, A. Yamaguchi, T. Kusumoto. *Mol. Cryst. liq. Cryst.*, **411**, 201 (2004).

[6] K. Ema, H. Yao, Y. Takanishi, H. Takezoe, T. Kusumoto, T. Hiyama, A. Yoshizawa. *Liq. Cryst.*, **29**, 221 (2002).
[7] Y. Maeda, M. Koizumi. *Rev. sci. Instrum.*, **67**, 2030 (1996); Y. Maeda, M. Koizumi. *Rev. high press. Sci. Technol.*, **7**, 1532 (1998).
[8] Y. Maeda, H. Kanetsuna. *Bull. Res. Inst. Polym. Tex.*, **149**, 119 (1985); Y. Maeda. *Thermochim. Acta.*, **163**, 211 (1990).
[9] Y. Maeda. In *Comprehensive Handbook of Calorimetry and Thermal Analysis*, T. Atake, T. Hashimoto, A. Inaba, S. Kidokoro, M. Oguni, R. Ozao, K. Saito, T. Tsuji, H. Yokokawa, H. Yoshida (Eds), pp. 386–388, John Wiley, New York (2004).
[10] Y. Maeda, G.-P. Cheng, S. Kutsumizu, S. Yano. *Liq. Cryst.*, **28**, 1785 (2001).
[11] Y. Maeda, K. Morita, S. Kutsumizu. *Liq. Cryst.*, **30**, 157 (2003).
[12] Y. Takanishi, T. Ogasawara, A. Yoshizawa, J. Umezawa, T. Kusumoto, T. Hiyama, K. Ishikawa, H. Takezoe. *J. mater. Chem.*, **12**, 1325 (2002).
[13] Y. Matsunaga, K. Hori, A. Yoshizawa, T. Kusumoto. *Liq. Cryst.*, **28**, 1805 (2001).
[14] Y. Maeda, T. Ito, S. Kutsumizu. *Liq. Cryst.*, **31**, 623 (2004).
[15] Y. Maeda, T. Ito, S. Kutsumizu. *Liq. Cryst.*, **31**, 807 (2004).